PHILOSOPHICAL TRANSACTIONS OF THE ROYAL SOCIETY A MATHEMATICAL, PHYSICAL & ENGINEERING SCIENCES

Sensitive Enzyme Electrodes [and Discussion]

W. John Albery, Martyn G. Boutelle, Sally L. T. Durrant, Marrianne Fillenz, Andrew R. Hopkins, Bernard P. Mangold, A. G. Fogg and G. S. Wilson

Phil. Trans. R. Soc. Lond. A 1990 **333**, 49-61
doi: 10.1098/rsta.1990.0136

Sensitive enzyme electrodes

By W. John Albery[1], Martyn G. Boutelle[2], Sally L. T. Durrant[3], Marrianne Fillenz[2], Andrew R. Hopkins[3] and Bernard P. Mangold[3]

[1] *Physical Chemistry Laboratory, University of Oxford, South Parks Road, Oxford OX1 3QZ, U.K.*

[2] *Department of Physiology, University of Oxford, Parks Road, Oxford OX1 3PT, U.K.*

[3] *Department of Chemistry, Imperial College of Science, Technology and Medicine, London SW7 2BZ*

Conventional enzyme electrodes are relatively insensitive devices capable of measuring analytes in the micromolar range. Inhibited enzyme electrodes work by measuring the inhibition of an enzyme turning over undersaturated conditions. This increased turnover gives greater sensitivity. The detection limits are controlled either by the thermodynamic amplitude or by the kinetic discrimination. Software has been developed to analyse the current time transient to produce concentrations of the inhibitor. Results for CN^- and H_2S are presented. The packed bed wall jet electrode is an electrode assembly that allows complete reaction of the substrate with the enzyme coupled to an efficient hydrodynamic régime for electrochemical detection. Results for the determination of acetylcholine are presented. The electrode can also be used in an immunoassay for the determination of human immunoglobulin in the nanomolar range. Finally results will be presented for *in vivo* changes in ascorbate in the brain of the freely moving rat as a result of tail pinch; changes on a timescale of half a second can be followed.

1. Introduction

One of the most fruitful marriages of the past few years has been that between enzymes and electrochemistry. Enzymes have evolved to recognize their substrates and can therefore be used to select the substrate from a complicated solution such as a biological fluid without the need for the traditional separation procedures of analytical chemistry. In the traditional enzyme electrode the rate of the enzyme reaction is proportional to the concentration of the substrate. The rate of this reaction is then transduced into current on a suitable electrode. Various strategies have been devised for this transduction. For instance Hill and Higgins (Cass *et al.* 1984) pioneered the use of inorganic mediators such as different sorts of Ferrocene, while we have developed the use of conducting organic salts (Albery *et al.* 1985*a*, 1986, 1987). In these direct amperometric electrodes the limits of detection are usually governed by the size of the unwanted background current. Interference from electroactive impurities means that it is difficult to measure concentrations below 1 μmol dm^{-3}. In this paper we describe a number of techniques for increasing the sensitivity of enzyme electrodes so that concentrations in the nanomolar range and trace amounts as low as femtomoles can be measured.

Phil. Trans. R. Soc. Lond. A (1990) **333**, 49–61

Printed in Great Britain

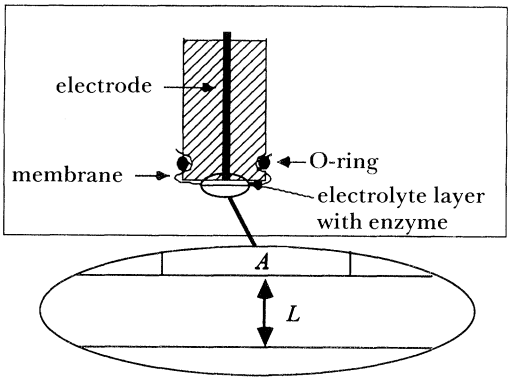

Figure 1. A conventional enzyme electrode of area A with an electrolyte layer of thickness L.

2. Inhibition enzyme electrodes

A typical membrane enzyme electrode is illustrated in figure 1. The enzyme is trapped in a thin electrolyte layer by dialysis membrane or for small gas molecules by a thin teflon membrane. The target analyte diffuses through the membrane and reacts with the enzyme in the thin electrolyte layer. The rate of the enzyme reaction is transduced into current using one of the strategies discussed above. One of the problems of achieving high sensitivity with the conventional amperometric membrane electrode (figure 1) is that the enzymatic reaction is confined to a thin layer of electrolyte. At low analyte concentrations the current is given by

$$i = nFALk_2[\mathrm{S}][\mathrm{E}]. \tag{1}$$

Using typical values of $i = 1\,\mathrm{nA}$, $nA = 1\,\mathrm{cm}^2$, $L = 1\,\mu\mathrm{m}$ and $[\mathrm{E}] = 1\,\mathrm{nmol\,cm}^{-3}$ we find that $k_2[\mathrm{S}]$ must equal $10^{-1}\,\mathrm{s}^{-1}$. If k_2 was a diffusion-controlled rate constant then one could measure S in the nanomolar range. However k_2 for most enzymes is more often *ca.* $10^6\,\mathrm{dm}^3\,\mathrm{mol}^{-1}\,\mathrm{s}^{-1}$ or less. Hence it will be difficult to obtain sufficient current from the conventional membrane electrode.

(*a*) *Theoretical model*

In the direct amperometric method one measures a current produced by obtaining one or two electrons from each molecule of target substrate. At low concentration the current is so small that it is swamped by the unwanted background current. However, greater sensitivity can be obtained if for instance a toxic molecule inhibits an enzyme. With each enzyme molecule turning over at say one thousand times a second, the binding of a single inhibitor molecule switches off these thousand molecular events per second. This leads to 'enzyme amplification'. We have recently published a complete theoretical description of this effect (Albery *et al.* 1990*a*). For the purposes of this paper we can simplify the scheme to that given below:

$$\mathrm{E} \xrightarrow{k_{\mathrm{cat}}} \mathrm{I} + \mathrm{E} \underset{k_{-\mathrm{I}}}{\overset{k_{\mathrm{I}}}{\rightleftharpoons}} \mathrm{EI}.$$

We assume that there is sufficient substrate so that the enzyme is saturated; the binding and release of the inhibitor are controlled by the rate constants k_{I} and $k_{-\mathrm{I}}$ respectively. The current, i, is given by:

$$i = nFALk_{\mathrm{cat}}[\mathrm{E}], \tag{2}$$

where n is the number of electrons, A is the area of the electrode and L is the thickness of the electrolyte layer trapped behind the membrane (figure 1).

Suppose that the concentration of inhibitor suddenly increases, then the formation of inhibited enzyme, EI, results in a drop in the concentration of E. The kinetics are given by

$$\mathrm{d[E]}/\mathrm{d}t = -k_{\mathrm{I}}[\mathrm{E}][\mathrm{I}] + k_{-\mathrm{I}}[\mathrm{EI}] = -[\mathrm{E}]\{k_{\mathrm{I}}[\mathrm{I}] + k_{-\mathrm{I}}\} + k_{-\mathrm{I}}[\mathrm{E}]_{\Sigma}, \tag{3}$$

where

$$[\mathrm{E}]_{\Sigma} = [\mathrm{E}] + [\mathrm{EI}]. \tag{4}$$

The current, i_0, before the arrival of the inhibitor is given by

$$i_0 = nFALk_{\mathrm{cat}}[\mathrm{E}]_{\Sigma}. \tag{5}$$

Inspection of (2) shows that on the arrival of I the concentration of E follows first-order kinetics with a rate constant $(k_{\mathrm{I}}[\mathrm{I}] + k_{-\mathrm{I}})$ as E falls to its final value, $[\mathrm{E}]_{\infty}$, given by

$$[\mathrm{E}]_{\infty} = [\mathrm{E}]_{\Sigma}/\{1 + k_{\mathrm{I}}[\mathrm{I}]/k_{-\mathrm{I}}\}. \tag{6}$$

In our previous work (Albery *et al.* 1987) we showed that this kinetic scheme was obeyed. However, in developing a toxic gas sensor it is not a sensible strategy to rely on following the kinetics of a reaction to completion: the toxic gas might interfere fatally with the analysis of the data before it was completed! We therefore rearrange (3) and use (2) and (5) so that it provides us at any time with a measurement of [I]:

$$[\mathrm{I}] = (k_{-\mathrm{I}}/k_{\mathrm{I}})(i_0/i - 1) + (1/k_{\mathrm{I}})[-\mathrm{d}\ln(i)/\mathrm{d}t]. \tag{7}$$

It is interesting that in this equation the second term is dominant at short times and the first term at long times.

(*b*) *Detection limits*

Before describing experimental results using (7) we will use the equation to estimate the sensitivity of these devices. We distinguish between those systems where the binding is reversible and $k_{-\mathrm{I}}$ is significant and those systems where the binding is so irreversible that $k_{-\mathrm{I}}$ is virtually equal to zero. For the reversible systems the inhibitor, I, must cause a detectable change in the current. If we take the percentage change to be 10% then both from (6) and the first term in (7) we find that the limits of measurement would be given by

$$[\mathrm{I}]_{\mathrm{L}} = 0.10/K_{\mathrm{I}}, \tag{8}$$

where $K_{\mathrm{I}} = k_{\mathrm{I}}/k_{-\mathrm{I}}$ is the binding constant for the inhibitor. The larger this constant the more sensitive is the sensor. We have pointed out before (Albery *et al.* 1987) that this means that the more toxic is the gas, the more sensitive is the sensor. The condition in (8) ensures that there is sufficient 'thermodynamic amplitude' for the sensor to work.

Turning to the irreversible case, the first term in (7) is now negligible and so we are depending on the second kinetic term. We will have to be able to see an increased decline in the current caused by I as opposed to the inevitable drift downwards in the absence of I. Let this drift be characterized by a first-order rate constant k_{D}. Then assuming that the arrival of I must make at least a 10% change in the rate, we find from (7) that

$$[\mathrm{I}]_{\mathrm{L}} = 0.10k_{\mathrm{D}}/k_{\mathrm{I}}. \tag{9}$$

This condition ensures that there is sufficient 'kinetic discrimination' for the sensor to work.

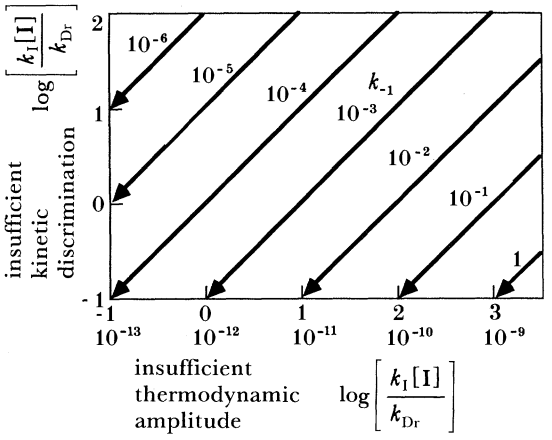

Figure 2. Case diagram showing how the detection limit for an inhibition enzyme electrode depends on the kinetic parameters. The diagram is drawn for $k_D = 10^{-4}$ s^{-1} and $K_I = 10^9$ dm^3 mol^{-1} s^{-1}.

We can now construct a 'case diagram' to display values of $[I]_L$. We assume first that $k_D = 10^{-4}$ s^{-1}, which implies that the enzyme is stable for several hours; smaller values of k_D would lead to better results. Secondly, since in most cases $K_I \gg 1$, we assume for the moment that k_I is a diffusion controlled reaction with a rate constant of 10^9 dm^3 mol^{-1} s^{-1}; a smaller value of k_I would lead to less good results. Figure 2 then displays a contour diagram, where each 45° line represents a value of the third rate constant k_{-I}. Lowering the value of [I] reduces both y and x and therefore involves travelling towards the SW corner on the appropriate 45° line. If $k_{-I} < k_D$, then the 45° line comes to an end when it intersects the left-hand margin, which is the condition for kinetic discrimination given by (9). On the other hand if $k_{-I} > k_D$, then the limiting condition is given by the horizontal line at the bottom of the diagram, which is the condition for sufficient thermodynamic amplitude given by (8). Although to construct figure 2 we have chosen particular values, the pattern displayed is a general one; the relative sizes of k_{-I} and k_D will determine whether the sensitivity of the system is limited by kinetic discrimination or by thermodynamic amplitude. With the chosen values it can be seen that inhibited enzyme electrodes are capable of being very sensitive devices. In practice k_I will probably be smaller than the diffusion controlled rate and so the devices will be less sensitive.

(*c*) *Cytochrome oxidase system*

The particular system that we have studied (Albery *et al.* 1987, 1990*b*, *c*) involves the respiratory enzyme cytochrome oxidase, E, which undergoes the following cycle of reactions with oxygen and cytochrome c, C:

$$\mathrm{E(red)} + \mathrm{O_2} \rightarrow \mathrm{E(ox)} + \mathrm{H_2O_2},$$

$$\mathrm{E(ox)} + \mathrm{C(red)} \rightarrow \mathrm{E(red)} + \mathrm{C(ox)}.$$

We then use a modified gold electrode (Albery *et al.* 1990*b*) to reduce C(ox) to C(red), thereby measuring the activity of the enzyme.

We have developed the necessary software to handle the data according to (7). One of the advantages of (7) is that the activity of the enzyme is measured using i_0. Hence the whole device is self-calibrating. The decrease in activity of the enzyme through

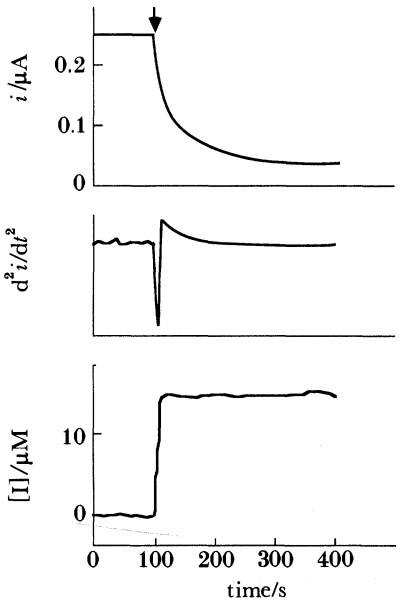

Figure 3. Typical results for the current, the second differential and [I] calculated from (7) for addition of CN^-.

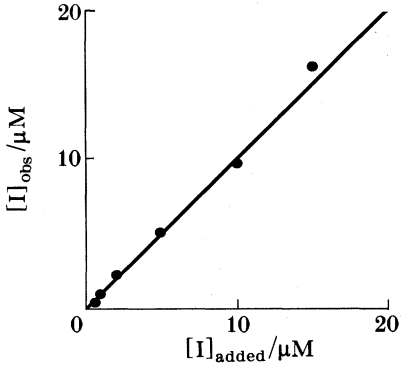

Figure 4. Calibration plot for CN^-.

natural drift does not matter. The arrival of I will cause d^2i/dt^2 to go sharply negative. We use this feature to trigger the measurement; the value of i_0 is then taken from the value of i just before d^2i/dt^2 went negative. Hence to find [I] using (7) we only need values for the rate constants k_I and k_{-I} and the measured quantities i_0, i, and $d\ln(i)/dt$. Values of the required rate constants can be measured relatively easily (Albery *et al.* 1990*b*). An important feature of the technique is that the analysis does not require us to know [E] or L or to control the enzyme kinetics. In figure 3 we show typical plots of i, d^2i/dt^2 and [I] calculated from (7) for the addition of CN^-. It is very satisfactory that within 20 s the value of [I] rises to a steady value long before the transient is completed. typical calibration plots for CN^- and H_2S are displayed in figures 4 and 5.

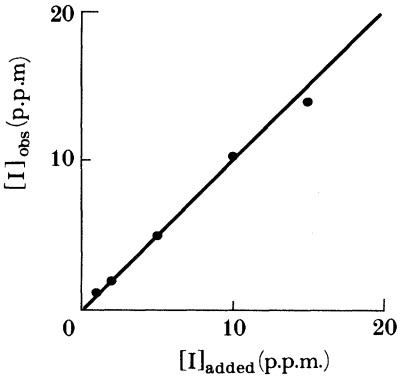

Figure 5. Calibration plot for H_2S.

3. Packed bed wall jet electrodes

(a) *Sensitivity of the packed bed wall jet electrode*

An alternative strategy for increasing the sensitivity is to use flow injection analysis with an electrochemical detector. For this purpose we have developed the packed bed wall jet electrode illustrated in figure 6 (Albery *et al.* 1985*b*). The wall jet electrode is constructed so that solution flowing through a small jet impinges on the circular disc electrode giving a known pattern of controlled hydrodynamics. Not only are the hydrodynamics controlled, but also compared with other electrode configurations a much higher percentage of the analyte (7–10 %) reaches the electrode surface (Albery & Brett 1983); therefore this hydrodynamic régime is the preferred one for trace analysis. Enzymes can be easily immobilized on the packed bed that is upstream of the jet (figure 6).

The geometry of the bed and the volume flow rate, V_f, determine t_B the time of contact a substrate molecule has with the bed of area A and length l:

$$t_B = Al/V_f. \tag{10}$$

Ideally we wish this time to be long enough for there to be complete reaction of the substrate. The fraction converted, f, is given by

$$f = 1 - \exp\{-k_2[E]t_B\}. \tag{11}$$

This argues for a slow flow rate. As opposed to this a slow flow rate gives a lower limiting current on the wall jet electrode ($i \propto V_f^{\frac{3}{4}}$) and more time for the sample to spread giving a lower peak height. The decrease in peak height by diffusional spreading is given by

$$p = \mathrm{erf}[(k_B t_B)^{-\frac{1}{2}}], \tag{12}$$

where k_B is given by

$$k_B = 4DA^2/V_S^2. \tag{13}$$

D is the diffusion coefficient of the substrate and V_S is the volume of the sample. For maximum sensitivity we require both f and p to be as close to unity as possible and this means that the geometry of the bed and V_f should be chosen so that

$$(3k_B)^{-1} > t_B > 3\{k_2[E]\}^{-1}. \tag{14}$$

Using typical values of $D = 10^{-5}\,\mathrm{cm^2\,s^{-1}}$ and $A = 0.50\,\mathrm{cm^2}$ we find that k_B ranges from $10^{-5}\,\mathrm{s^{-1}}$ for $V_S = 1$ ml to $10^{-1}\,\mathrm{s^{-1}}$ for $V_S = 10$ µl. Hence depending on the sample size to satisfy (14) we require $k_2[E] > 10^{-4}\,\mathrm{s^{-1}}$ for $V_S = 1$ ml or $> 1\,\mathrm{s^{-1}}$ for $V_S = 10$ µl. These conditions for the enzyme kinetics are easier to achieve than those associated

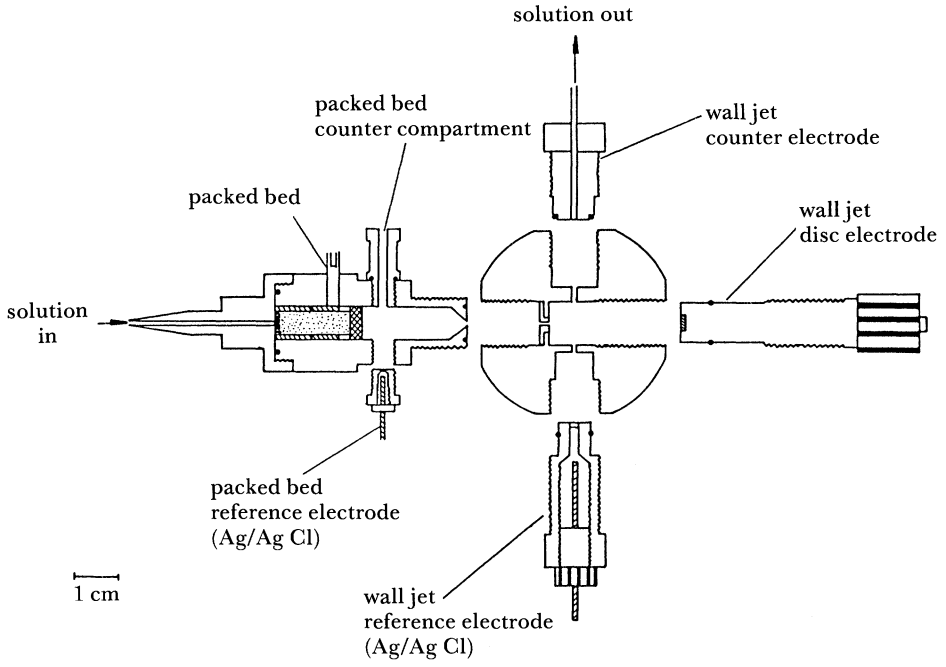

Figure 6. A packed bed wall jet electrode. The packed bed can either be an electrode, as illustrated, or can be enzyme loaded beads.

with (1). For most systems we can design the bed so as to achieve 100% conversion and yet retain a sharp peak.

Assuming a typical conversion factor for the wall jet electrode of 10% the current will be given by

$$i = nF(0.10)\, V_f\, [S].$$

With i as before equalling 1 nA and a typical V_f of 0.10 $cm^3\ s^{-1}$ we find that we will obtain sufficient current when [S] is 1 nmol dm^{-3}. There is also a further advantage in that the peak in current from flow injection analysis discriminates against the background current. Hence we conclude that the packed bed wall jet electrode is inherently more sensitive than a membrane enzyme electrode.

(*b*) *Acetylcholine assay*

We now describe how using this technique we can measure very low levels of acetylcholine. We are interested in the natural levels of acetylcholine in the extracellular fluid of the brain of the freely moving rat. The ambient concentration in the brain fluid is less than nanomolar. We use the powerful new technique of microdialysis (Ungerstedt 1986). A small dialysis probe is inserted into a specific brain region. Ringer solution flows continuously through the probe; the aceylcholine diffuses across the dialysis membrane and is thereby extracted and collected in the laboratory. We find that 25 min of collection will typically yield 12 fmoles of acetylcholine.

Our assay uses three coupled enzyme reactions on the packed bed. First, we use acetylcholine esterase to turn acetylcholine into choline:

$$\text{acetylcholine} \xrightarrow[\text{esterase}]{\text{acetylcholine}} \text{choline}.$$

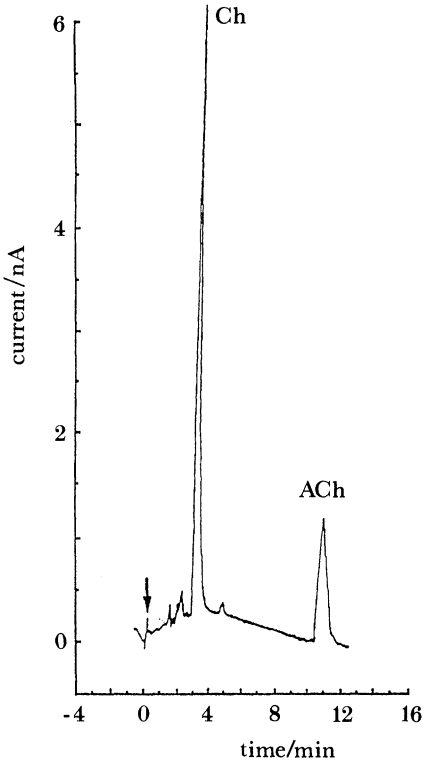

Figure 7. Typical results from dialysate using the packed bed wall jet electrode for choline (Ch) and acetylcholine (ACh).

The choline is then oxidized by choline oxidase to betaine:

$$2O_2 + \text{choline} \xrightarrow{\text{choline oxidase}} \text{betaine} + 2H_2O_2.$$

Many historic enzyme assays would then detect H_2O_2 electrochemically. This practice is not to be recommended, because the electrochemistry of H_2O_2 is badly behaved. We advocate a procedure developed by Hill (Frew *et al.* 1986) in which H_2O_2 is consumed by horseradish peroxidase producing the well behaved and much beloved ferricinium ion, Fcp^+:

$$H_2O_2 + 2Fcp \xrightarrow{\text{horseradish peroxidase}} H_2O + 2Fcp^+. \qquad (16)$$

The packed bed contains three sections in which the three enzymes sequentially produce $4Fcp^+$ for every original acetylcholine molecule. The ferricinium ion is easily reduced on a glassy carbon wall jet electrode; the mild potential required to do this minimizes problems associated with unwanted background currents or interference from other electroactive compounds extracted in the dialysate.

Typical results are shown in figure 7. In this case an HPLC column was used to separate choline from acetylcholine. The well-formed peak for acetylcholine corresponds to the collection of 12 fmol. We estimate that amounts as low as 0.1 fmol can be measured by this technique. In figure 8 we show results from a

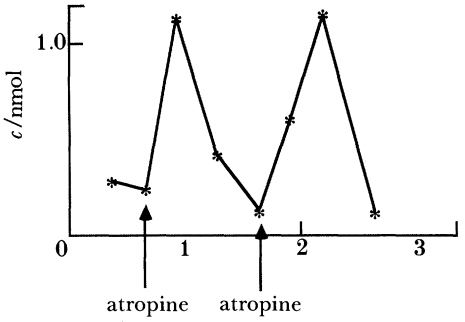

Figure 8. The effect on acetylcholine levels in the striatum of the brain of a freely moving rat of adding atropine, an inhibitor of acetylcholine esterase.

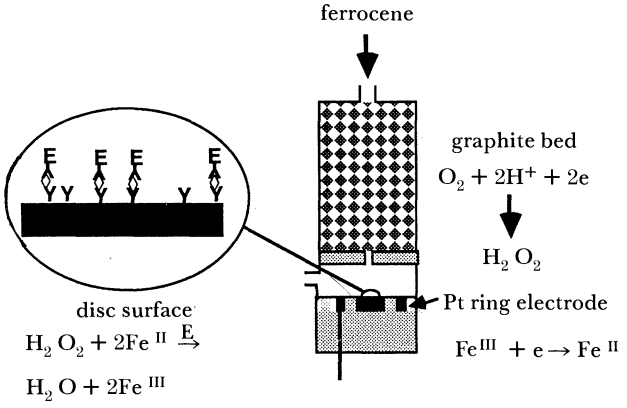

Figure 9. The packed bed wall jet electrode immunoassay.

typical neurophysiological experiment in which the local application of atropine has inhibited the acetylcholine esterase in the brain resulting in the observed rise in acetylcholine.

(*c*) *An immunoassay*

We have shown that the packed bed wall jet electrode can be used as an electrochemical detector in a sensitive immunoassay for human immunoglobulin G (IgG). Goat anti-human IgG (Y) was immobilized on the glassy carbon disc of a wall jet electrode. The usual 'sandwich' procedure was then followed. The electrode was first dipped into a buffer containing a known amount of human IgG◇:

(17)

The electrode was then exposed to goat anti-human IgG that had been labelled with horseradish peroxidase E:

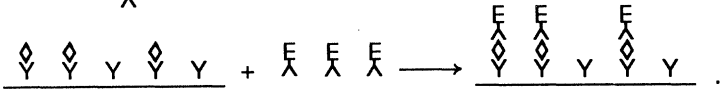

The wall jet electrode was then fitted into the packed bed assembly illustrated in figure 9. As shown in (16) the enzyme requires two substrates. The ferrocene was supplied in the flowing buffer while the H_2O_2 was generated electrochemically on the

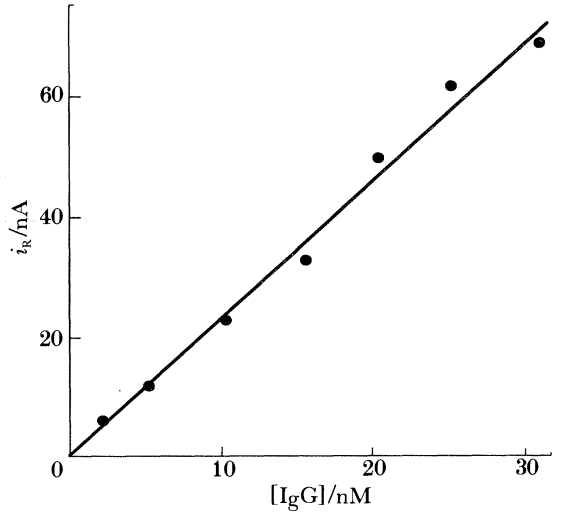

Figure 10. Calibration plot for the packed bed wall jet electrode immunoassay.

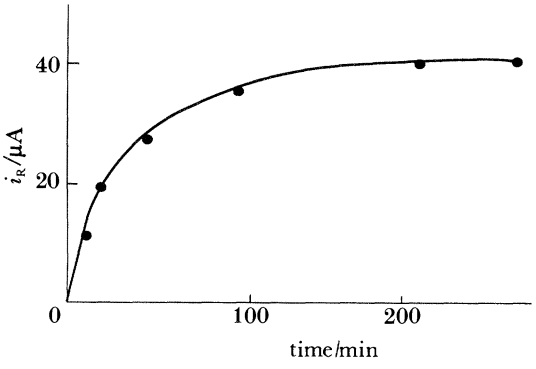

Figure 11. The slow kinetics of the binding of the antigen in the immunoassay.

packed bed electrode. Taking advantage of the wall jet ring disc hydrodynamics (Albery & Brett 1983), the ferricinium ion produced by the enzyme was measured on the downstream ring electrode. The advantage of the electrochemical generation of H_2O_2 is that by switching the packed bed electrode on and off one can distinguish on the ring electrode between the background current and the current due to the enzyme-generated ferricinium ion. This discrimination means that one can reliably measure 1 nA of current caused by the enzyme.

A calibration plot is shown in figure 10. It can be seen that nanomolar concentrations of IgG can be measured. Figure 11 shows the effect on the current of varying the incubation time of reaction (17). The binding reaction is rather slow. The results in figure 10 were obtained with 15 min incubation. Greater sensitivity could be achieved by giving the reaction time to go to completion.

Two features of this approach should be emphasized. The use of the packed bed electrode to discriminate against background currents and the use of the ring electrode to measure the ferricinium ion in the diffusion layer before it becomes diluted in the bulk of the solution. With a ring current of 1 nA corresponding to a flux of 10^{-14} mol s^{-1} and an enzyme turning over at 10^3 s^{-1} it can be seen that it is

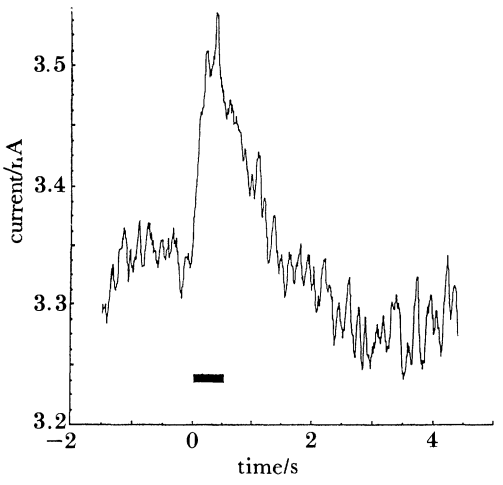

Figure 12. The rapid response of an *in vivo* electrode measuring ascorbate to a half second tail pinch. The time that the forceps were applied is shown by the black bar.

possible to measure 10^{-17} moles of material on the disc. The reason for this enhanced sensitivity compared to the conventional membrane electrode is that in the sandwich immunoassay the enzyme can be driven as fast as possible under saturated conditions, while in the conventional electrode the enzyme is only being turned over by a low concentration of the target analyte.

4. *In vivo* determination of ascorbate

Our final example describes the use of an implanted *in vivo* electrode to follow the variation of ascorbate with time in the brain of the freely moving rat (Boutelle *et al.* 1989). It is believed that ascorbate levels are linked to the firing of neuronal pathways involving the neurotransmitter, glutamate. Unlike acetylcholine, ascorbate is the most abundant electroactive compound in the extracellular fluid. There is therefore no need to use an enzyme to discriminate in favour of this particular compound. However, we are interested in measuring small changes in ascorbate levels in response to behavioural stimuli.

Hitherto it has been customary to measure ascorbate using linear sweep voltammetry (Albery *et al.* 1984). We have shown that after several days the implanted electrode is surrounded by glial cells which form a sampling compartment. The linear sweep technique consumes all of the ascorbate in the compartment; one then has to wait *ca.* 10 min for fresh ascorbate to replenish the compartment. In behavioural studies better time resolution would be desirable. The current from the continuous oxidation of ascorbate as it diffuses into the compartment will be much smaller than the peak current observed in linear sweep where the ascorbate has accumulated for minutes. To measure the smaller continuous current we have designed and developed a high quality potentiostat. One feature of our design is the isolation of all circuits involving the mains from the electrochemical DC circuits. This potentiostat can be used to measure currents as low as 100 fA.

Typical results for the chemical response to a half second tail pinch are shown in figure 12. When the tail is squeezed gently, the ascorbate rises; on releasing the tail it starts immediately to fall. It should be pointed out that the amplitude of the spike

is less than 10% of the total ascorbate current and this is another reason for requiring a high quality potentiostat. It is somewhat ironic that our original *in vivo* ascorbate measurements involved the elaborate technique of semidifferentiation; this was then replaced by the much simpler linear sweep, which in its turn has been superseded by the simplest amperometric technique of all, constant potential voltammetry. The direct measurement of the chemical changes shown in figure 12 in response to such mild behavioural stimuli will lead us to a much greater understanding of the molecular chemistry of behaviour and memory. The work also emphasizes an advantage of electrochemical sensing in that the rat does not have to be vaporized or subjected to ultra high vacuum.

We thank the SERC, the MRC, the Wolfson Foundation and the Leverhulme Trust for financial support.

References

Albery, W. J. & Brett, C. M. A. 1983 The wall-jet ring-disc electrode. Part 1: theory. *J. electroanal. Chem.* **148**, 201–210.

Albery, W. J., Bartlett, P. N. & Cass, A. E. G. 1987 Amperometric enzyme electrodes. *Phil. Trans. R. Soc. Lond.* B **316**, 107–119.

Albery, W. J., Bartlett, P. N., Bycroft, M., Craston, D. H. & Driscoll, B. J. 1986 Amperometric enzyme electrodes. 3. A conducting salt electrode for the oxidation of four different flavoenzymes. *J. electroanal. chem.* **218**, 119–126.

Albery, W. J., Bartlett, P. N. & Craston, D. H. 1985*a* Amperometric enzyme electrodes. 2. Conducting salts as electrode materials for the oxidation of glucose oxidase. *J. electroanal. Chem.* **194**, 223–245.

Albery, W. J., Cass, A. E. G., Mangold, B. P. & Shu, Z. X. 1990*c* Inhibited enzyme electrodes. Part 3: a sensor for low levels of H_2S and HCN. *Biosensors Bioelectron.* **5**, 397–413.

Albery, W. J., Cass, A. E. G. & Shu, Z. X. 1990*a* Inhibited enzyme electrodes. Part 1: theoretical model. *Biosensors Bioelectron.* **5**, 367–378.

Albery, W. J., Cass, A. E. G. & Shu, Z. X. 1990*b* Inhibited enzyme electrodes. Part 2: The kinetics of the cytochrome oxidase system. *Biosensors Bioelectron.* **5**, 379–395.

Albery, W. J., Goddard, N. J., Beck, T. W., Fillenz, M. & O'Neill, R. D. 1984 Theoretical and experimental studies of linear sweep voltammetry in the rat brain. *J. electroanal. Chem.* **161**, 221–233.

Albery, W. J., Haggett, B. G. D., Jones, C. P., Pritchard, M. J. & Svanberg, L. R. 1985*b* The packed bed wall-jet electrode and the determination of NO_3^-. *J. electroanal. Chem.* **188**, 257–263.

Boutelle, M. G., Svennson, L. & Fillenz, M. 1989 Rapid changes in striatal ascorbate in response to tail pinch monitored by constant potential voltammetry. *Neurosci.* **30**, 11–17.

Cass, A. E. G., Davies, G., Francis, G. D., Hill, H. A. O., Aston, W. J., Higgins, I. J., Plotkin, E. V., Scott, L. D. L. & Turner, A. P. F. 1984 Ferrocene mediated enzyme electrode for amperometric determination of glucose. *Analyt. Chem.* **57**, 667–671.

Frew, J. E., Harmer, M. A., Hill, H. A. O. & Libor, S. I. 1986 A method of estimation of hydrogen peroxide based on mediated electron transfer reactions of peroxidases at electrodes. *J. electroanal. Chem.* **201**, 1–12.

Ungerstedt, U. 1986 Microdialysis – a new bioanalytical sensing technique. *Current Separations* **7**, 43–46.

Discussion

A. G. Fogg (*Loughborough University of Technology, U.K.*). Exactly what kind of electrode was used to measure the small charges in ascorbic acid? Was it a carbon fibre electrode?

W. J. Albery. In fact it was a carbon paste electrode made with silicone oil.

G. S. Wilson (*The University of Kansas, U.S.A.*). The rather slow reaction between Professor Albery's immobilized antibody (on carbon electrode) and the antigen probably has two causes. First, the mass transfer conditions are quite unfavourable. We have shown that in a flowing stream (reactor column) the AbAg reaction is complete in a matter of a few seconds. Secondly, the orientation of the Ab on the surface also affects the reaction rate. These problems can be corrected. More serious, however, is the affect of non-specific interactions. The coverage of a surface with Ab yields about 10^{-12} mole cm^{-2}. Non-specific effects can be 1–10% of this figure meaning that at low levels the detection limit is defined by non-specific interactions and *not* by the intrinsic sensitivity of the detector method.

W. J. Albery. Thank you.

PHILOSOPHICAL TRANSACTIONS OF THE ROYAL SOCIETY A MATHEMATICAL, PHYSICAL & ENGINEERING SCIENCES